Biophysical Journal Volume 98 March 2010 743–752

Harmonic Oscillations in Homeostatic Controllers: Dynamics of the p53 Regulatory System

Ingunn W. Jolma,[†] Xiao Yu Ni,[†] Ludger Rensing,[‡] and Peter Ruoff[†*]
[†]Centre for Organelle Research, University of Stavanger, Stavanger, Norway; and [‡]Department of Biology, University of Bremen, Bremen, Germany

ABSTRACT Homeostatic mechanisms are essential for the protection and adaptation of organisms in a changing and challenging environment. Previously, we have described molecular mechanisms that lead to robust homeostasis/adaptation under inflow or outflow perturbations. Here we report that harmonic oscillations occur in models of such homeostatic controllers and that a close relationship exists between the control of the p53/Mdm2 system and that of a homeostatic inflow controller. This homeostatic control model of the p53 system provides an explanation why large fluctuations in the amplitude of p53/Mdm2 oscillations may arise as part of the homeostatic regulation of p53 by Mdm2 under DNA-damaging conditions. In the presence of DNA damage p53 is upregulated, but is subject to a tight control by Mdm2 and other factors to avoid a premature apoptotic response of the cell at low DNA damage levels. One of the regulatory steps is the Mdm2-mediated degradation of p53 by the proteasome. Oscillations in the p53/Mdm2 system are considered to be part of a mechanism by which a cell decides between cell cycle arrest/DNA repair and apoptosis. In the homeostatic inflow control model, harmonic oscillations in p53/Mdm2 levels arise when the binding strength of p53 to degradation complexes increases. Due to the harmonic character of the oscillations rapid fluctuating noise can lead, as experimentally observed, to large variations in the amplitude of the oscillation but not in their period, a behavior which has been difficult to simulate by deterministic limit-cycle models. In conclusion, the oscillatory response of homeostatic controllers may provide new insights into the origin and role of oscillations observed in homeostatically controlled molecular networks.

INTRODUCTION

Mechanisms that maintain robust homeostasis in genetic and biochemical networks are essential for the fitness of organisms in a changing and challenging environment (1). Many physiologically important variables are under tight homeostatic control, where internal concentrations or fluxes are maintained at well-defined levels despite environmental perturbations. Such perfect adaptation/homeostasis (2) has been found, for example, in bacterial chemotaxis (3–6), photoreceptor responses (7), and MAP-kinase regulation (8–10). Drengstig et al. (11) have recently shown how perfect adaptation motifs may be identified in reaction kinetic networks.

Although perfect homeostasis can be related to the control-theoretic concepts of integral feedback or integral control (12,13), it has recently been shown that, in reaction kinetic terms, perfect homeostasis is closely connected to the presence of a zero-order flux (14), which controls another controlling agent (i.e., control of the controller). The latter is responsible for the removal or synthesis of a homeostatically regulated intermediate. Fig. 1 shows two controller motifs from Ni et al. (14), in which intermediate A is homeostatically regulated. Fig. 1 *a* presents an inflow controller, where the control mechanism can compensate for large in-flow perturbations of A, and Fig. 1 *b* presents an outflow-controller, where A shows homeostasis when A is subject to large fluctuations in its removal. It should be noted that these control schemes will generally fail, when large outflows occur in inflow controllers or large inflows occur in outflow controllers (14).

Here, we demonstrate that the two homeostatic controllers in Fig. 1 can show damped or practically undamped large amplitude harmonic oscillations. The degree of damping depends on the binding characteristics between the controller E_{adapt} and A, as well as on the synthesis and removal of the homeostatically controlled intermediate A. To our knowledge, this is the first example that describes large amplitude harmonic oscillations in a biochemical oscillator model (see the recent review on design principles of biochemical oscillators (15)).

Interestingly, the controller in Fig. 1 *a* shows high similarity to the feedback control of p53 by Mdm2, when A is taken as p53, E_{adapt} as Mdm2, and E_{tr} as the class of Mdm2-independent proteasomal degradation reactions of p53 (16–21). In the presence of DNA damage, p53 is upregulated by slowing down its various degradation reactions, but still requires a tight control to avoid premature apoptosis by high levels of p53 (22,23). We propose the idea that this control is mediated by Mdm2 and related factors by means of a homeostatic inflow mechanism, which maintains a level of p53 in a state of indecisiveness, until a final decision between cell cycle arrest/DNA repair and apoptosis is made (24). Oscillations in p53/Mdm2 (25,26) may participate in making this decision. In the proposed inflow model, harmonic

Submitted August 15, 2009, and accepted for publication November 11, 2009.

*Correspondence: peter.ruoff@uis.no

Editor: Andre Levchenko.

0006-3495/10/03/0743/10 $2.00

doi: 10.1016/j.bpj.2009.11.013

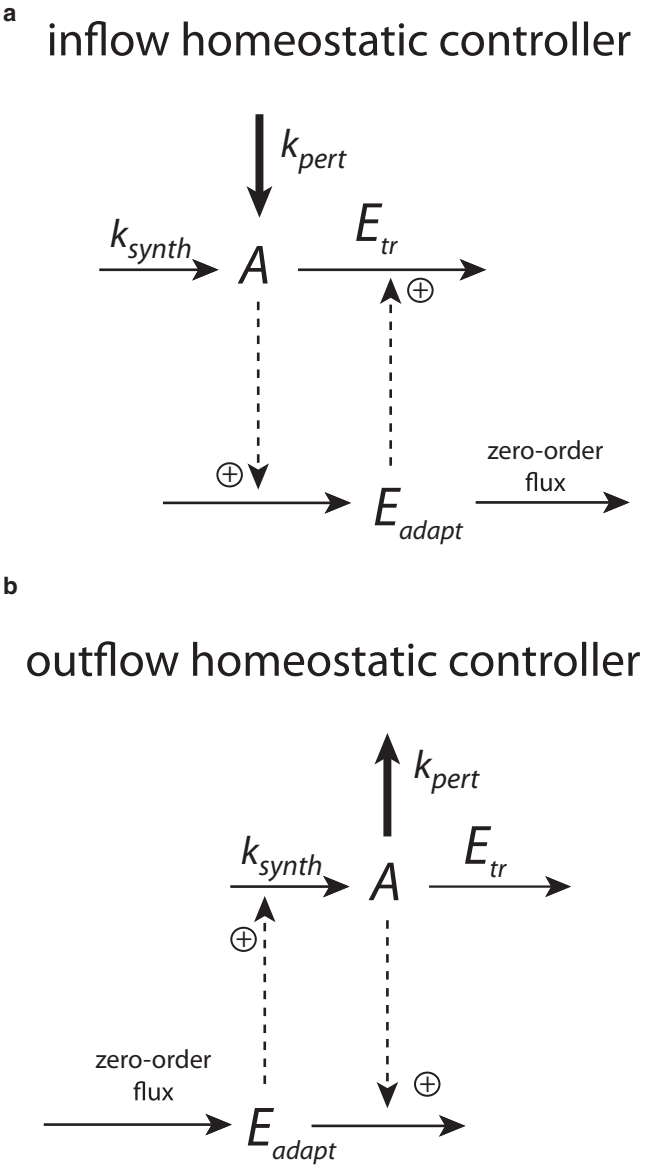

FIGURE 1 Schemes of inflow (*a*) and outflow (*b*) homeostatic controllers in which component *A* shows robust homeostasis against environmentally uncontrolled perturbations in the inflow and outflow of *A* (14). E_{adapt} represents an enzyme important in the adaptation/homeostasis of *A*, E_{tr} represents one or several enzymes important in transforming/removing *A*, and k_{synth} is a rate constant associated with the synthesis of *A*. Thick solid arrows with k_{pert} indicate where in the controller inflow or outflow perturbations occur. For a more detailed discussion of these schemes, see Ni et al. (14).

oscillations in p53 and Mdm2 can occur when p53 binds strongly to the Mdm2-induced degradation machinery, where p53 oscillates around the level defined by the homeostatic controller. Due to the harmonic character of the oscillation, rapid molecular noise leads to large variations in the p53/Mdm2 amplitude whereas the period is only little affected—a behavior that has been experimentally observed (27) but which is difficult to reproduce by deterministic limit-cycle models (27,28). Large fluctuating amplitudes in the p53/Mdm2 oscillations seem to be of importance in determining cell fate (26,27), as will be discussed in more detail below. Thus, a homeostatic inflow model provides an integrative view on the negative feedback regulation of p53 and the appearance of oscillations. Such a view may also provide new insights into the origin and role of oscillations observed in homeostatically controlled molecular networks.

Harmonic oscillations in perfect controllers

A possible kinetic representation for the inflow-controller scheme of Fig. 1 *a* can be given by

$$\frac{dA}{dt} = k_{pert} + k_{synth} - k \cdot E_{adapt} A^{n} - \frac{V_{max}^{E_{tr}} A}{K_M^{E_{tr}} + A}, \quad (1)$$

$$\frac{dE_{adapt}}{dt} = k_{adapt} A - \frac{V_{max}^{E_{set}} E_{adapt}}{K_M^{E_{set}} + E_{adapt}}, \quad (2)$$

where $V_{max}^{E_i} = k_{cat}^{E_i} E_i^{tot}$ with $k_{cat}^{E_i}$ and E_i^{tot} is the turnover number and total concentration of enzyme species *i*, respectively. The *n* is the reaction order with respect to *A* in the removal of *A* by E_{adapt}. With respect to the discussion that will follow below, it may be noted that zero-order kinetics with respect to A ($n = 0$ in Eq. 1) may be obtained by

$$\frac{k \cdot E_{adapt} \cdot A}{K_M^{E_{adapt}} + A} \rightarrow k \cdot E_{adapt}, \quad (3)$$

when $K_M^{E_{adapt}} \ll A$. In terms of a rapid equilibrium model of the Michaelis-Menten equation, small $K_M^{E_{adapt}}$ values can be interpreted as a strong affinity between substrate *A* and E_{adapt}.

The set-point for homeostatic regulation in *A* is determined by setting Eq. 2 to zero and demanding that the controller E_{adapt} is removed by another control species (E_{set}) under zero-order conditions. This requires that $K_M^{E_{set}} \ll E_{adapt}$, which gives the homeostatic set-point A_{set} for *A* at steady-state conditions (14):

$$A_{set} = \frac{V_{max}^{E_{set}}}{k_{adapt}} = \frac{k_{cat}^{E_{set}} E_{set}^{tot}}{k_{adapt}}. \quad (4)$$

A is robustly regulated as long as the right-hand term of Eq. 4 remains practically constant and as long the degradation in *A* is not dominating with respect to the influxes k_{pert} and k_{synth}. In Eq. 2, the removal of E_{adapt} by E_{set} using Michaelis-Menten kinetics also ensures that, even at low $K_M^{E_{set}}$ values, E_{adapt} does not become negative, as it sometimes would if the A_{set} term $(V_{max}^{E_{set}} E_{adapt})/(K_M^{E_{set}} + E_{adapt})$ were to be replaced by a true constant (14).

An interesting aspect is that oscillations emerge in the controller when the reaction order becomes zero with respect to *A*. Fig. 2 illustrates this behavior by applying a stepwise change in k_{pert} (from 1.0 to 2.0) when the system is initially at a steady state at first and zero reaction orders with

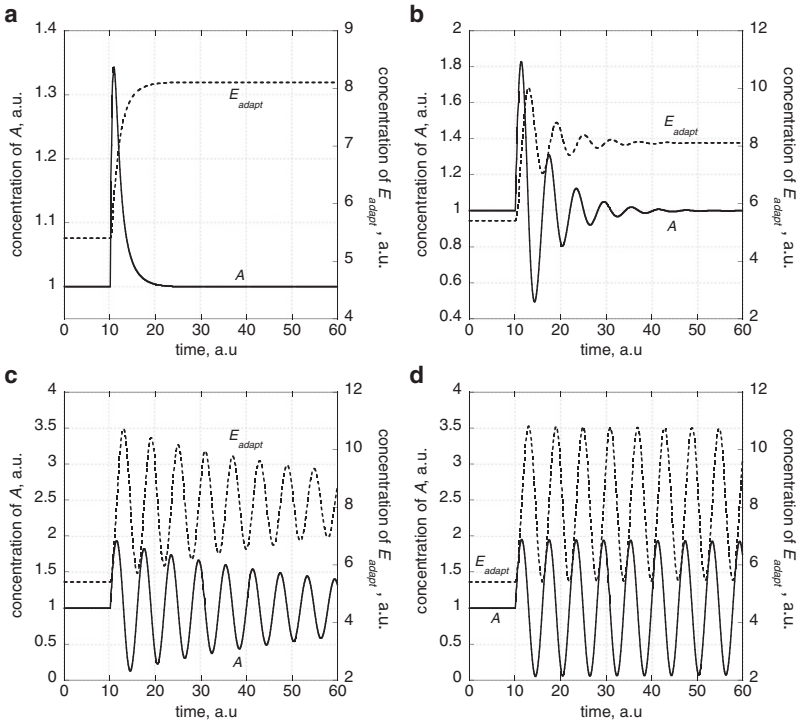

FIGURE 2 Generation of harmonic oscillations for the homeostatic controller in Fig. 1 *a* by decreasing reaction order n with respect to A. Rate constant values are $k_{\text{pert}} = 1.0$, $k_{\text{adapt}} = 3.0$, $k_{\text{cat}}^{E_{\text{set}}} = 6 \times 10^6$, $K_{\text{M}}^{E_{\text{set}}} = 1 \times 10^{-6}$, $k_{\text{synth}} = 1.0$, $k_{\text{cat}}^{E_{\text{tr}}} = 1 \times 10^2$, and $K_{\text{M}}^{E_{\text{tr}}} = 1 \times 10^2$ with $A_{\text{set}} = 1.0$. The reaction orders n with respect to A are (*a*) 1.0; (*b*) 1×10^{-1}; (*c*) 1×10^{-2}; and (*d*) 0.0. At time $t =$ 10.0 a.u., k_{pert} is increased from 1.0 to 2.0 and the system approaches a new steady state. Note that A shows robust homeostasis with $A_{\text{set}} = 1.0$. With decreasing n values harmonic oscillations are emerging where A oscillates around A_{set} with a peak amplitude approaching A_{set} as n approaches zero.

respect to A. By using the rate constant values described in Fig. 2 such that the term $V_{\text{max}}^{E_{\text{tr}}} A/(K_{\text{M}}^{E_{\text{tr}}} + A)$ in Eq. 1 can be neglected and assuming zero-order kinetics with respect to A, we can approximate Eqs. 1 and 2 by Eq. 5,

$$\frac{\ddot{A}}{k \cdot k_{\text{adapt}}} + A = A_{\text{set}}, \tag{5}$$

which leads to undamped harmonic oscillations in A and E_{adapt} with a period length $P = 2\pi/(k \cdot k_{\text{adapt}})$.

A kinetic representation of the outflow control scheme of Fig. 1 *b* can be described as

$$\frac{dA}{dt} = k_{\text{synth}} + k \cdot E_{\text{adapt}} - \frac{V_{\text{max}}^{E_{\text{tr}}} A}{\left(K_{\text{M}}^{E_{\text{tr}}} + A\right)}, \tag{6}$$

$$\frac{dE_{\text{adapt}}}{dt} = j_0 - \frac{V_{\text{max}}^{E_{\text{set}}} E_{\text{adapt}} A}{\left(K_{\text{M}}^{E_{\text{set}}} + E_{\text{adapt}}\right)}. \tag{7}$$

In this formulation, the controller shows an oscillatory response in A and E_{adapt} for moderate k_{synth} values and for low values in $K_{\text{M}}^{E_{\text{tr}}}$ and $K_{\text{M}}^{E_{\text{set}}}$, i.e., having a zero-order degradation of A in Eq. 6 and a first-order degradation rate of E_{adapt} with respect to A in Eq. 7. In the following we will focus on the inflow controller scheme of Fig. 1 *a* as a simple model for the p53 regulatory system and its oscillatory behavior.

Regulation of p53

The p53 system is one of the most complex regulatory networks known (22,24,29–35). It is involved in the control of cell cycle, senescence, DNA repair, apoptosis, and the prevention of tumor development. More than half of all human tumors contain mutations of the p53 gene and in almost all tumors the p53 regulatory circuit is nonfunctional (31,32). Normally (i.e., in the absence of DNA damaging conditions), p53 levels are low due to a rapid degradation by ubiquitin-dependent and ubiquitin-independent pathways with an approximate p53 half-life between 6 and 30 min (16–21,36,37). An important regulator of p53 is Mdm2, an E3 (ubiquitin) ligase for p53 and other tumor suppressors (38,39). p53 activates the transcription of Mdm2, which binds p53 (40), ubiquitinates it, and thus initiates the proteasomal degradation of p53 both in the nucleus and cytosol (41). This is the central autoregulatory (negative) feedback loop of p53 (29,32). In the presence of DNA damage or oxidative stress, p53 is upregulated by several mechanisms that inhibit Mdm2 activity (42), increase Mdm2 autodegradation (43), and inhibit p53 degradation (44,45). This leads either to cell cycle arrest and DNA repair at lower DNA damage, or to the induction of programmed cell death (apoptosis) at higher DNA damage (24,46,47).

Interestingly, in the presence of high DNA damage, p53 and Mdm2 have been found to oscillate (25–27,48–50). The origin and purpose of these oscillations is little understood, but may be of considerable interest (26,50,51).

We became interested in the feedback regulation of the p53/Mdm2 system and its oscillatory response because it shows a close analogy to the inflow homeostatic control scheme shown in Fig. 1 *a* with $A \equiv$ p53 and $E_{\text{adapt}} \equiv$ Mdm2. The control scheme suggests that, under DNA-damaging

conditions, p53 is homeostatically regulated to a certain upper level defined by Mdm2 (and other factors), at which it decides on the essential cellular functions mentioned above. This view is supported by the fact that transgenic mice, which lack both Mdm2 and p53, grow up normally, whereas mice lacking only Mdm2 die as embryos, possibly due to the uncontrolled apoptotic activity of p53 (22,23).

Once p53 is regulated to a high level, harmonic oscillations can occur when p53 binds strongly to ternary or multiprotein complexes/scaffolds containing Mdm2 (52–54), which are involved in the (proteasomal) degradation of p53. In the presence of rapidly fluctuating molecular noise, the harmonic character of the p53/Mdm2 oscillations leads to a large variability in their amplitudes but not in their frequency, as will be shown below. This property is difficult to simulate by limit cycle models (28). At normal conditions, i.e., in the absence of DNA damage, p53 is rapidly degraded by ubiquitin-dependent and ubiquitin-independent processes, keeping p53 levels well below its upper limits.

Fig. 3 *a* shows an outline of a simple inflow regulatory circuit for the p53-Mdm2 system. A kinetic representation of this model can be given by the following equations:

$$\frac{d\mathrm{p53}}{dt} = k_{\mathrm{s}}^{\mathrm{p53}} - \frac{k'C_0}{\frac{K_{\mathrm{A}}\cdot K_{\mathrm{AB}}}{\mathrm{p53}\cdot\mathrm{Mdm2}} + \frac{K_{\mathrm{AB}}}{\mathrm{Mdm2}} + \frac{K_{\mathrm{BA}}}{\mathrm{p53}} + 1} - \frac{V_{\max}^{E_{\mathrm{d}}}\mathrm{p53}}{K_{\mathrm{M}}^{E_{\mathrm{d}}} + \mathrm{p53}} - k_{\mathrm{s}}^{\mathrm{p53^*}}\mathrm{p53} + k_{\mathrm{r}}^{\mathrm{p53^*}}\mathrm{p53^*}, \quad (8)$$

$$\frac{d\mathrm{Mdm2}}{dt} = k_{\mathrm{s}}^{\mathrm{Mdm2}}\mathrm{p53} - \frac{V_{\max}^{E_{\mathrm{set}}}\mathrm{Mdm2}}{K_{\mathrm{M}}^{E_{\mathrm{set}}} + \mathrm{Mdm2}} - k_{\mathrm{s}}^{\mathrm{Mdm2^*}}\mathrm{Mdm2} + k_{\mathrm{r}}^{\mathrm{Mdm2^*}}\mathrm{Mdm2^*}, \quad (9)$$

$$\frac{d\mathrm{p53^*}}{dt} = k_{\mathrm{s}}^{\mathrm{p53^*}}\mathrm{p53} - k_{\mathrm{r}}^{\mathrm{p53^*}}\mathrm{p53^*} - k_{\mathrm{d}}^{\mathrm{p53^*}}\mathrm{p53^*}, \quad (10)$$

$$\frac{d\mathrm{Mdm2^*}}{dt} = k_{\mathrm{s}}^{\mathrm{Mdm2^*}}\mathrm{Mdm2} - k_{\mathrm{r}}^{\mathrm{Mdm2^*}}\mathrm{Mdm2^*} - k_{\mathrm{d}}^{\mathrm{Mdm2^*}}\mathrm{Mdm2^*}. \quad (11)$$

The Mdm2-mediated degradation term in Eq. 8 is based on a rapid equilibrium among p53, Mdm2, and a protein complex/scaffold *C* as illustrated in Fig. 3 *b* (and described in more detail in the Supporting Material). C_0 denotes the total concentration of *C*, and K_{A}, K_{B}, K_{AB}, and K_{BA} are dissociation (K_{M}) constants. Due to the "Principle of Detailed Balance" (55), we have $K_{\mathrm{A}} \cdot K_{\mathrm{AB}} = K_{\mathrm{B}} \cdot K_{\mathrm{BA}}$. Low values in the K_{i} values indicate strong binding and stable complexes. Zero-order kinetics in p53 can be achieved by low K_{A} and K_{BA} values, whereas first-order kinetics with respect to Mdm2 is obtained for relative large K_{AB} values. Applying these conditions, we get

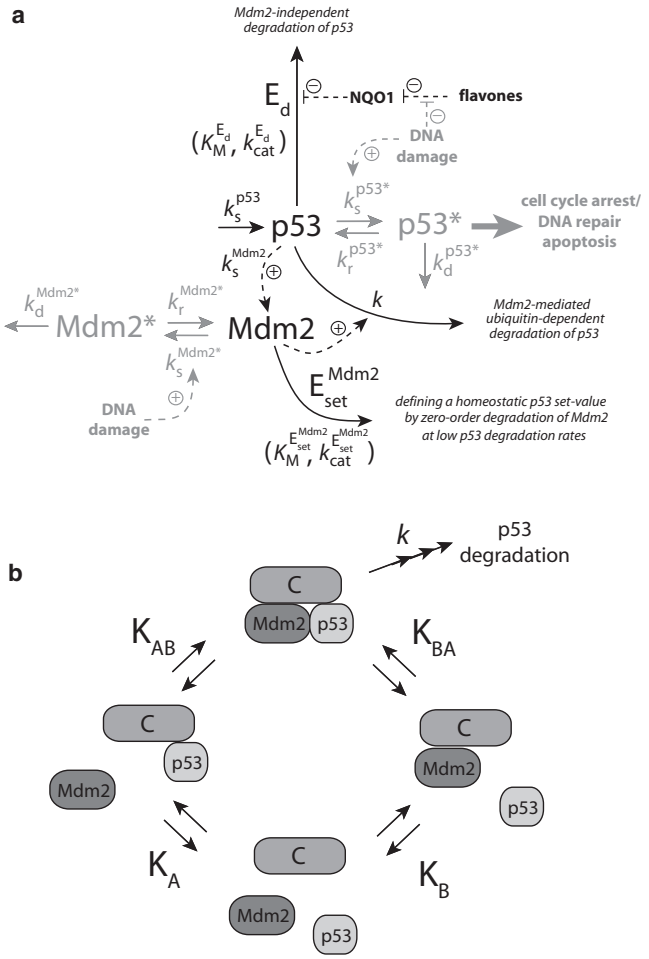

FIGURE 3 (*a*) The p53-Mdm2 negative feedback system as a homeostatic inflow control model. Reactions outlined in black occur in the absence of DNA damage. Under latter conditions, p53 is considered to be rapidly removed through Mdm2 and through Mdm2-independent proteasomal degradation. The Mdm2-independent degradation processes are represented in the model by E_{d} with Michaelis-Menten parameters $K_{\mathrm{M}}^{E_{\mathrm{d}}}$ and $k_{\mathrm{cat}}^{E_{\mathrm{d}}}$. $E_{\mathrm{set}}^{\mathrm{Mdm2}}$ is an enzyme or a class of enzymes involved in the degradation of Mdm2. When this degradation becomes zero-order with respect to Mdm2, then p53 shows robust homeostatic regulation to the set-point $\mathrm{p53_{set}} = (k_{\mathrm{cat}}^{E_{\mathrm{set}}^{\mathrm{Mdm2}}} E_{\mathrm{set,\,tot}}^{\mathrm{Mdm2}})/k_{\mathrm{s}}^{\mathrm{Mdm2}}$. However, due to rapid p53 degradation at normal conditions, p53 levels are well below $\mathrm{p53_{set}}$. In the presence of DNA damage the degradation of p53 is slowed down and p53 is stabilized. One of the stabilizing mechanisms involve upregulation of NQO1 (16,19,20). Due to the zero-order degradation of Mdm2 by $E_{\mathrm{set}}^{\mathrm{Mdm2}}$, p53 levels are limited by the set-value $\mathrm{p53_{set}}$ (see Fig. 4, *a* and *b*). When the removal of p53 induced by Mdm2 becomes zero-order with respect to p53, harmonic oscillations in p53 and Mdm2 are generated (see Fig. 4, *c* and *d*). p53* and Mdm2* represent posttranslational modification species of p53 and Mdm2, respectively. There is evidence that the modified forms p53* and Mdm2* do interact much less (30,35). In the model, p53* and Mdm2* are assumed to be in rapid equilibrium with p53 and Mdm2, respectively. (*b*) Molecular mechanism in the Mdm2-mediated degradation which can lead to zero-order kinetics with respect to p53 and first-order kinetics with respect to Mdm2. p53 and Mdm2 bind to a protein complex/scaffold C, which leads to the ubiquitination and degradation in p53. A strong binding of p53 to the complex (small K_{A} and K_{BA} values) lead to zero-order kinetics with respect to p53, whereas a relative weak binding of Mdm2 lead to first-order kinetics with respect to Mdm2. For details, see main text and the Supporting Material.

$$\frac{k'C_0}{\frac{K_A K_{AB}}{\text{p53}\cdot\text{Mdm2}}+\frac{K_{AB}}{\text{Mdm2}}+\frac{K_{BA}}{\text{p53}}+1}\rightarrow\frac{k'C_0}{K_{AB}}\text{Mdm2}=k\cdot\text{Mdm2}. \tag{12}$$

In Fig. 3 *a*, the outline in black shows the functioning of the system in the absence of DNA damage. p53 is held at low levels due to degradation through a Mdm2-mediated ubiquitin-dependence and Mdm2-independent proteasomal degradations (16–20,36,37).

Under DNA-damaging conditions, p53 is upregulated and posttranslationally modified. One of the processes that lead to an increase in p53 is the Mdm2-independent upregulation of NADH quinone oxidoreductase 1 (NQO1) (16). NQO1 binds to p53 and thereby stabilizes it (56). Both p53 and Mdm2 undergo posttranslational modifications (22,57), where phosphorylated and acetylated forms are indicated in the model by p53* and Mdm2*. These forms interact much less than unmodified forms of Mdm2 and p53 and thus cause a stabilization of p53. Due to the decrease in the Mdm2-independent degradation of p53 under DNA damaging conditions but due to the presence of the (still operative) zero-order kinetic degradation of unmodified p53 by unmodified Mdm2, harmonic oscillations of p53 and Mdm2 are initiated, and subsequently propagated to the posttranslationally modified forms p53* and Mdm2*. In addition, MdmX has been shown to bind to both Mdm2 and p53, which stabilizes each of these species (58). In our model, the stabilization of Mdm2 and p53 by MdmX is lumped together with the formation of the Mdm2* and p53* species. However, it should be noted that MdmX is also present in undamaged cells and considered to maintain transcriptionally inactive p53 in the nucleus of these cells (58).

Fig. 4 shows concentration profiles for p53 and Mdm2 using the model Eqs. 8–11 with decreasing rates in the ubiquitin-independent degradation of p53 when the Mdm2-mediated degradation of p53 is zero-order with respect to p53. Large degradation rates in p53 through E_d lead to p53 levels well below $p53_{set}$ (Fig. 4 *a*),

$$\text{p53}_{\text{set}}=\left(k_{\text{cat}}^{E_{\text{set}}^{\text{Mdm2}}}E_{\text{set, tot}}^{\text{Mdm2}}\right)\Big/k_{\text{s}}^{\text{Mdm2}}, \tag{13}$$

whereas p53 levels become homeostatically regulated when the E_d-induced degradation becomes sufficiently low (Fig. 4 *b*). At even lower E_d-mediated degradation of p53, damped oscillations appear (Fig. 4 *c*), where p53 oscillates around $p53_{set}$ with a peak amplitude, which (in the absence of noise) cannot exceed $p53_{set}$ (Fig. 4 *d*).

Amplitude/frequency behavior and influence of noise

The damping of the oscillations given by Eqs. 8–11 depends on several parameters. A strong damping or no oscillatory response is observed when p53 or the posttranslationally modified species Mdm2* or p53* are rapidly degraded, i.e., when rate constants $k_{\text{cat}}^{E_d}$, $k_{\text{d}}^{\text{p53}^*}$, or $k_{\text{d}}^{\text{Mdm2}^*}$ are large compared to the influx of p53. On the other hand, sustained oscillations are observed when $k_{\text{cat}}^{E_d}$, $k_{\text{d}}^{\text{p53}^*}$, or $k_{\text{d}}^{\text{Mdm2}^*}$ are much lower than the influx of p53 into the controller. When $k_{\text{s}}^{\text{p53}^*}$

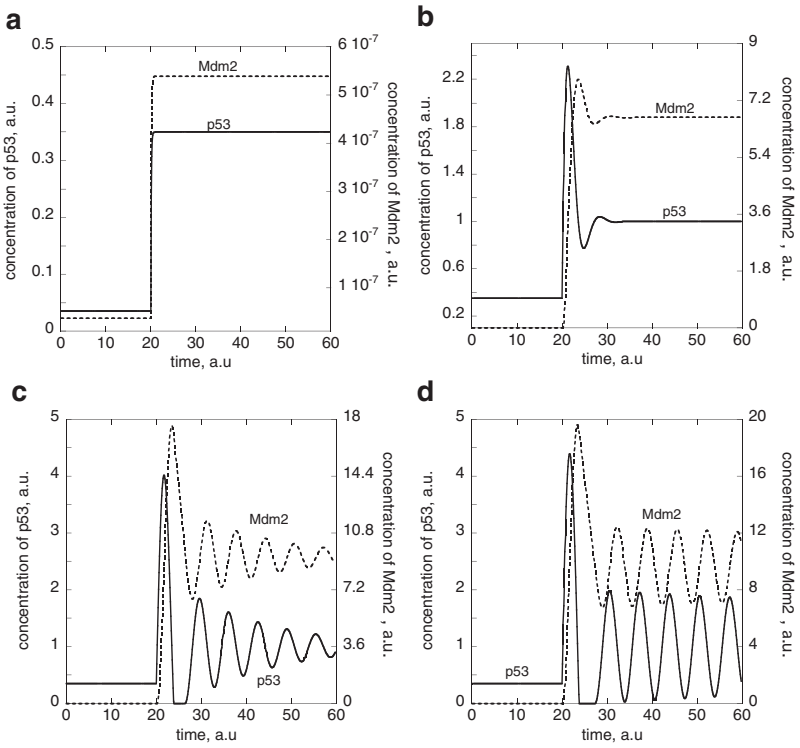

FIGURE 4 Generation of harmonic oscillations for the homeostatic inflow controller of the p53-Mdm2 system by upregulating p53, i.e., by successively decreasing the $k_{\text{cat}}^{E_d}$ value of the Mdm2-independent degradation of p53 (see Fig. 3 and Eqs. 8–11). Rate constant values (in a.u.) are as follows: $k_{\text{s}}^{\text{p53}}=3.5$, $K_A\cdot K_{AB}=1.0\times10^{-4}$, $K_{AB}=1.0\times10^{2}$, $K_{BA}=1.0\times10^{-7}$, $k'\cdot C_0=40.0$, $k_{\text{s}}^{\text{Mdm2}}=3.0$, $k_{\text{cat}}^{E_{\text{set}}^{\text{Mdm2}}}=6.0\times10^{6}$, $K_{\text{M}}^{E_{\text{set}}^{\text{Mdm2}}}=1.0\times10^{-6}$, $K_{\text{M}}^{E_d}=1.0\times10^{4}$, $k_{\text{r}}^{\text{p53}*}=50.0$, $k_{\text{d}}^{\text{p53}*}=0.0$, $k_{\text{r}}^{\text{Mdm2}*}=1.0\times10^{2}$, $k_{\text{d}}^{\text{Mdm2}*}=0.0$, $E_{\text{set, tot}}^{\text{Mdm2}}=5.0\times10^{-7}$, $E_{\text{d, tot}}=0.1$, and $p53_{set}=1.0$. (*a*) High values of $k_{\text{cat}}^{E_d}$ lead to p53 steady-state values well below its homeostatic set-value $p53_{set}$. At $t=20$ time units $k_{\text{cat}}^{E_d}$ is decreased from 1.0×10^{7} to 1.0×10^{6} with $k_{\text{s}}^{\text{p53}*}=k_{\text{s}}^{\text{Mdm2}*}=0.0$, which leads to an increase in the p53 and Mdm2 steady-state levels. (*b*) At $t=20$ time units, $k_{\text{cat}}^{E_d}$ is decreased from 1.0×10^{6} to 1.0×10^{5} with $k_{\text{s}}^{\text{p53}*}=k_{\text{s}}^{\text{Mdm2}*}=0.1$. Note that p53 attains now its homeostatic regulated set-value. (*c*) At $t=20$ time units, $k_{\text{cat}}^{E_d}$ is decreased from 1.0×10^{6} to 1.0×10^{4} with $k_{\text{s}}^{\text{p53}*}=k_{\text{s}}^{\text{Mdm2}*}=0.5$. Damped harmonic oscillations in p53 start to emerge around the homeostatic set-value. (*d*) At $t=20$ time units, $k_{\text{cat}}^{E_d}$ is decreased from 1.0×10^{6} to 1.0×10^{2} with $k_{\text{s}}^{\text{p53}*}=k_{\text{s}}^{\text{Mdm2}*}=1.0$. Much less damped harmonic oscillations in p53, p53*, Mdm2, and Mdm2* are generated (data for p53* and Mdm2* not shown).

and $k_s^{Mdm2^*}$ are zero, the system oscillates with the period $2\pi/(k \cdot k_s^{Mdm2})$. When $k_s^{p53^*}$, and $k_s^{Mdm2^*}$ are nonzero, sustained oscillations are also observed when $k_d^{p53^*}$ and $k_d^{Mdm2^*}$ are zero and a rapid equilibrium between p53* and p53 as well as Mdm2* and Mdm2 is established. The period increases as the rapid equilibrium is shifted more to the p53* and/or Mdm2* side. If the equilibrium between posttranslationally modified p53*/Mdm2* and unmodified p53/Mdm2 is slow compared with the influx of p53, oscillations become damped.

Fig. 5 shows trajectories of (practically) undamped oscillations in the p53-Mdm2 phase plane with different initial concentrations. Because the system is harmonic (conservative), no limit cycle is observed, but parallel trajectories emerge. In the case in which the trajectories reach the ordinate (Mdm2 axis when p53 = 0), Mdm2 concentrations decrease until an oscillator with maximum peak amplitude equal to the p53 set-value emerges (trajectory 5 in Fig. 5). One may consider such a behavior as a filtering of large excursions in p53 down to a maximum peak level determined by $p53_{set}$.

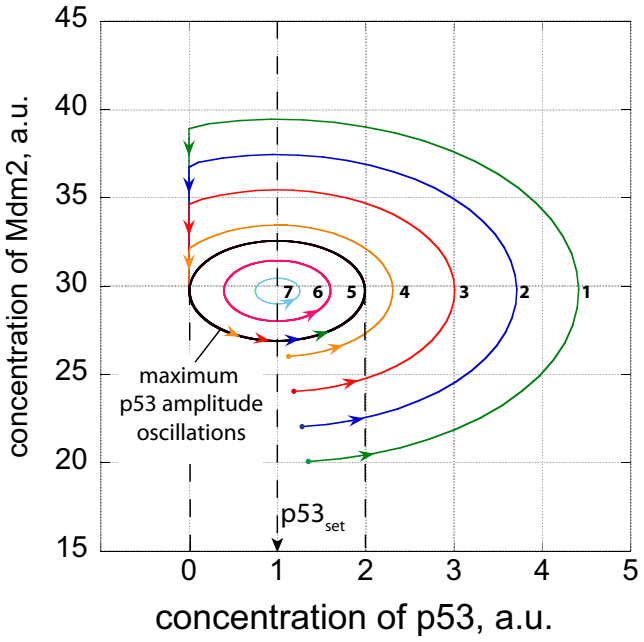

FIGURE 5 Phase plane trajectories of p53-Mdm2 harmonic oscillations going through three cycles. Rate constants as described in the legend of Fig. 4. To illustrate that k_s^{p53} can be chosen without affecting the p53 oscillations around $p53_{set}$, k_s^{p53} was set to 11.0, and $k_{cat}^{E_d} = 1.0 \times 10^2$. For the sake of simplicity, all $k_{s,\,r,\,d}^{p53*}$ and $k_{s,\,r,\,d}^{Mdm2*}$ rate constants are set to zero. Dots show different p53 and Mdm2 start concentrations. Because the system is conservative, parallel trajectories 1–7 emerge from each of the starting points. Trajectories 1–4 which lie outside of trajectory 5 (which is tangenting the ordinate at p53 = 0) will hit the ordinate at low p53 levels and Mdm2 concentrations will decrease until the system emerges as trajectory 5 oscillations, which have the largest peak amplitude equal to the p53 set-value. Trajectories 6 and 7 which start inside of trajectory 5 will not be altered, and the system oscillates with peak amplitudes lower than the p53 set-value.

The period is not affected by the remaining rate constants. Note that $k_{cat}^{E_d}$ needs to be sufficiently small and $K_M^{E_d}$ needs to be sufficiently large to get oscillations, but the period of the oscillations is not dependent on those values.

Due to the large amplitude variations found for experimentally recorded p53/Mdm2 oscillations (27), we became interested in the effect of fluctuations on the model. For this purpose, rate parameters were allowed to vary randomly and rapidly within a certain range by using the Fortran routine RAN1 (59). Fig. 6, *a* and *b*, shows the variations in k_s^{p53} and $k_{cat}^{E_d}$ as a function of time (see Supporting Material for an overview of all rate parameter variations). Fig. 6 *c* shows the behavior of the model compared to experimental data (Fig. 6 *d*). The computations show, in agreement with the experimental observations, that the amplitude of the oscillations is subject to considerable variation, whereas the period and the phase relationship between p53 and Mdm2 are little affected. However, it should be noted that changes in the average values of k (Eq. 12) or k_s^{Mdm2} will lead to period changes, because these two parameters determine period length (compare with Eq. 5).

DISCUSSION

p53 regulation: comparison with experiments

The homeostatic inflow model suggests the need for p53-regulation to avoid unregulated large p53 levels that would lead to premature apoptosis. An intriguing aspect of the p53-Mdm2 regulatory system is the occurrence of oscillations. There are two major requirements to get oscillations in the homeostatic inflow model:

1. The need for a relatively strong binding between p53 and the controller (Mdm2); and
2. That the degradation of p53 by Mdm2-independent processes (represented in the model by the E_d degradation pathway) should be low compared to the removal of newly synthesized p53 by Mdm2 (Eq. 8).

With respect to the first requirement, binding studies have shown that Mdm2 and p53 can interact by their N-terminal domains or by Mdm2's acid domain and p53's core domain (40). The latter binding site appears to be essential for the ubiquitination of p53 and its degradation. Ma et al. (60) estimated the dissociation constant (K_d) of this binding site as well as the K_M value of p53 from ubiquitination kinetics. They concluded that there is a relative high affinity ($<1\ \mu M$) between Mdm2 and p53 for this binding site, supporting the requirement by the homeostatic inflow model. Ma et al. further conclude that although the individual peptides derived from the acidic and zinc-finger domain of Mdm2 show a weak affinity toward p53 (40), there may be multiple contacts to form a specific site with higher affinity in binding to p53 within the central domain of Mdm2. With respect to the model's second requirement, experiments have shown

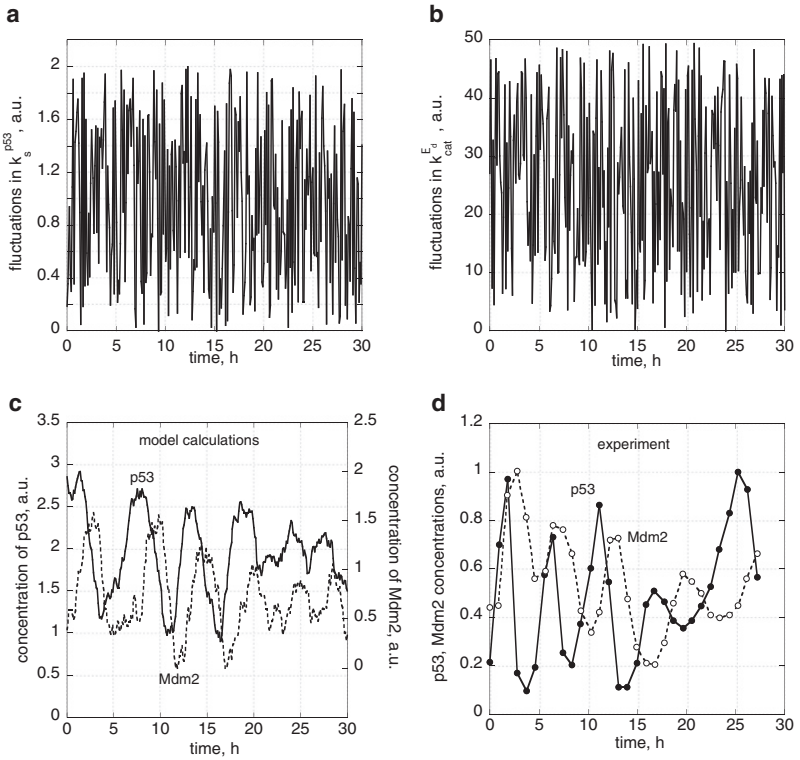

FIGURE 6 Rapid fluctuations in rate parameters lead to variations in the amplitude of the p53/Mdm2 oscillations, but preserve their period. For the sake of simplicity, all $k_{s,\,r,\,d}{}^{p53*}$ and $k_{s,\,r,\,d}{}^{Mdm2*}$ rate constants are set to zero. (*a* and *b*) Variations for k_s^{p53} and $k_{cat}^{E_d}$, respectively; see also Supporting Material. (*c*) Resulting oscillations in p53 and Mdm2 levels when applying rapid fluctuations for all rate parameters within the ranges indicated by Table S1 in the Supporting Material. Rate constant values of k and k_s^{Mdm2} have been adjusted such that the period of the harmonic unperturbed oscillations is close to the experimental value of 5.5 h (27). (*d*) Observed p53 (*solid line*) and Mdm2 (*dashed line*) oscillations in single cells. (Replotted from upper left of Fig. 1 *B* in Geva-Zatorsky et al. (27).)

that p53 becomes stabilized by a decrease in the Mdm2 stability (43) and by inhibiting Mdm2-independent degradation pathways (16–21,36,37). Although in the model oscillations with little damping can be observed when $k_{cat}^{E_d}$ is decreased to 10^2 a.u. (Fig. 4), $k_{cat}^{E_d}$ can practically be set to zero without significantly altering the oscillations, as long as there is some synthesis in p53.

The other parameters can be varied within a wide range during which oscillations can still be observed, and rate constant values (with timescales in hours, Fig. 6, *a–c*) can reflect observed half-lives for p53 and Mdm2 (43,61).

For getting p53 to be homeostatically controlled, Mdm2 (or other p53-degrading factors which constitute a negative feedback loop with p53) need to be removed by zero-order kinetics, i.e., at the maximum enzymatic activity for Mdm2 removal (14). It may be that accelerated MDM2 autodegradation (43) is a mechanism to reach maximum (zero-order) Mdm2 degradation and thus p53 homeostasis.

Due to the harmonic character of the model's oscillations, the phase difference between p53 and Mdm2 is given by the relationship $\pi/2$: $2\pi = \varphi$: P, where P is the period of the harmonic oscillator in the absence of posttranslational modifications. With an average experimental period of ~6 h (27), the calculated phase difference is ~1.5 h, which is in good agreement with the experimentally determined value of $2h \pm 0.5h$ (27). The period length P is dependent on two rate constants by $P = 2\pi/(k \cdot k_{adapt})$. This relationship is a good approximation. In the presence of posttranslational modifications of p53 and Mdm2, the period increases with increasing amounts of p53* and Mdm2*. Assuming rapid equilibria between p53*/Mdm2* and the respective unmodified forms p53/Mdm2, in the harmonic limit k_{adapt} is multiplied by a factor $f^{p53^*} = K^{p53^*}/(1 + K^{p53^*})$, with $K^{p53^*} = p53^*/p53$, whereas k is multiplied with a corresponding factor $f^{Mdm2^*} = K^{Mdm2^*}/(1 + K^{Mdm2^*})$ with $K^{Mdm2^*} = Mdm2^*/Mdm2$. Thus, in this representation of the p53 regulation the period of the oscillations should change when the ratio between posttranslationally modified p53/Mdm2 is altered. The model also implies that the source of oscillations is the presence of unmodified p53 and Mdm2, probably due to an undisturbed synthesis (22).

Geva-Zatorsky et al. (27) reported that not all cells show oscillations but that the fraction of oscillatory cells increase as the dose of the γ-irradiation increases. Our model suggests that with increasing dose of γ-irradiation and the subsequent lowering of the Mdm2-independent degradation of p53, oscillations appear when the Mdm2-induced removal of p53 is zero-order, with respect to p53. The damping of the oscillations is determined by several factors including the strength of p53-binding to the p53-degrading protein-complexes or scaffolds. When this binding is weak, our model predicts strong damping in the p53/Mdm2 oscillations, whereas the oscillations should become less damped when the binding to the p53-degrading protein complexes is strong. Other factors leading to damping or loss of the oscillations is a high (Mdm2-independent) p53 degradation rate and the accumulation of excess posttranslationally modified p53.

Significance of zero-order kinetics

Zero-order kinetics appear to be significant in several respects. In robust homeostatic controllers, zero-order fluxes define the set-values of (homeostatically) controlled variables (14), i.e., define the integral feedback (13) necessary for robust control. In the model presented here, zero-order flux in the degradation of Mdm2 suggests that p53 may be subject to robust control, such that its concentration is not able to exceed an upper boundary limit. This limit ($p53_{set}$, Eq. 13) is reached in the presence of DNA damage when the Mdm2-independent degradation reaction of p53 (16–21) is inhibited or slowed down by mechanisms still not well understood (Fig. 3). When, in addition to this upregulation of p53, the p53 reaction order in the Mdm2-mediated removal of p53 is zero due to a strong binding of p53 to its degradation complex, harmonic oscillations appear, whose peak amplitude is determined by $p53_{set}$ (Fig. 5). Due to the harmonic character of the oscillations, the amplitude of the p53/Mdm2 oscillations is quite sensitive to rapid perturbations/fluctuations similar to experimental observations (Fig. 6).

Biological significance

Do the oscillations and the large variability in the p53/Mdm2 amplitudes serve a purpose? One possibility may be that the oscillations represent a counting mechanism by which decisions are made whether DNA repair should be enhanced or apoptosis should be initiated (62). A higher number of cycles would favor apoptosis because higher p53 activity/concentration activates pro-apoptotic genes (63). A periodic activation of these genes may have the advantage of lowering inhibition actions at the promoter site or elsewhere—compared to continuous activation (64). This can be associated with a significant decrease in the threshold level of radiation at which the decision from pro-survival to pro-apoptotic state occurs (51). To make such a decision as unbiased as possible, the large variability in the p53 amplitudes seem to indicate that such fluctuations play a role in the p53 decision between ''life and death'' (46). Another possibility discussed for the role of oscillations is a longer maintenance of indecisiveness for a better evaluation of the pros and cons of a decision (26).

Besides defining the set-values of homeostatically controlled variables (14), zero-order reactions are also key elements in ultrasensitive switches (65–67). Although we have not considered such switches explicitly here, it is intriguing that zero-order kinetics can lead to such diverse behaviors ranging from ultrasensitive switches, relating homeostatic threshold values to oscillatory responses. It will be interesting to combine such regulatory motifs in regulatory models of biological networks.

Comparison with other models

Due to the importance of p53 in the control of DNA integrity, cell cycle arrest, and apoptosis, as well as its relevance for cancer research (48,49), a variety of models for the negative feedback control of p53 by Mdm2 and its oscillatory responses have been proposed (27,68–75). In contrast to the model presented here which shows harmonic oscillations, other models (27,68,70–74) are based on deterministic limit cycle oscillations. Several additional oscillator classes have recently been analyzed by Geva-Zatorsky et al. (27) and Zhang et al. (70). The model presented here is based on a homeostatic inflow control mechanism (14) when p53 becomes upregulated. This inflow controller can show harmonic oscillations, which are suppressed when p53 is normally at low levels due to several degradation mechanisms (16–21,36,37). Concerning the observed oscillations in the inflow controller, we are not aware of any molecular mechanism that has been shown to exhibit large amplitude harmonic oscillations. It may also be noted that the rapidly fluctuating molecular noise applied on rate parameters by RAN1 (Fig. 6, *a* and *b*, and Supporting Material) has practically an infinite period (59) and leads to large variations in the amplitude of the p53/Mdm2 oscillation (Fig. 6 *c*) in close agreement to experimental data (Fig. 6 *d*). With the exception of recent stochastic approaches (28,69,75) none of the deterministic models have presently been able to model the large variability in amplitude in the presence of rapid molecular fluctuations.

Since the pioneering work of Goodwin (76), many studies have shown that negative feedback regulation can lead to oscillations. The Goodwin equations (76) have been applied to circadian (77) as well as ultradian rhythms (73). In transcriptional-translational negative feedback regulators the intermediate mRNA species have been recognized to induce transcriptional time delays, which are important to generate these oscillations (73). In addition, protein (or mRNA) stabilities are important determinants for period length (78,79).

In this model the negative feedback involving the transcriptional and translational processes induced by p53 have been fused into the single first-order term $k_s^{Mdm2} \cdot p53$ (Eq. 9). This first-order term suggests that binding of p53 at the Mdm2 promoter is relatively weak, where k_s^{Mdm2} describes the overall expression of Mdm2 under such conditions (see Supporting Material).

The occurrence of large amplitude harmonic oscillations in cell regulatory networks, such as the oscillations in the core regulatory unit of the p53/Mdm2 system, appears intriguing. Similar highly variable amplitude oscillations with a relatively fixed frequency have been reported in the SOS DNA-damage response of *Escherichia coli* (80) and in the NF-κB system (81–83). Both NF-κB and the SOS regulation in *E. coli* are based on negative feedback regulation similar to the p53/Mdm2 system. Whether the variability in amplitude in the SOS or in NF-κB system can be based on similar oscillatory dynamics as found for homeostatic controllers (14) and considered here for the p53/Mdm2 system will be the subject of further investigations.

SUPPORTING MATERIAL

Description of computational methods, kinetics of scaffold-supported p53 and Mdm2 degradation, kinetics of p53 induced Mdm2 synthesis, and random variation of rate constants are available at http://www.biophysj.org/biophysj/supplemental/S0006-3495(09)01740-8.

P.R. thanks Jay Dunlap for hospitality while a revised version of the manuscript was prepared.

This research was supported in part by the Norwegian Research Council under grant No. 167087/V40 (to I.W.J.) and FUGE Systems Biology (SysMO) grant No. 183085/S10 (to X.Y.N.).

REFERENCES

1. Stelling, J., U. Sauer, …, J. Doyle. 2004. Robustness of cellular functions. *Cell*. 118:675–685.
2. Asthagiri, A. R., and D. A. Lauffenburger. 2000. Bioengineering models of cell signaling. *Annu. Rev. Biomed. Eng*. 2:31–53.
3. Berg, H. C., and P. M. Tedesco. 1975. Transient response to chemotactic stimuli in *Escherichia coli*. *Proc. Natl. Acad. Sci. USA*. 72:3235–3239.
4. Barkai, N., and S. Leibler. 1997. Robustness in simple biochemical networks. *Nature*. 387:913–917.
5. Alon, U., M. G. Surette, …, S. Leibler. 1999. Robustness in bacterial chemotaxis. *Nature*. 397:168–171.
6. Hansen, C. H., R. G. Endres, and N. S. Wingreen. 2008. Chemotaxis in *Escherichia coli*: a molecular model for robust precise adaptation. *PLoS Comput. Biol*. 4:0014–0027.
7. Ratliff, F., H. K. Hartline, and W. H. Miller. 1963. Spatial and temporal aspects of retinal inhibitory interaction. *J. Opt. Soc. Am*. 53:110–120.
8. Asthagiri, A. R., C. M. Nelson, …, D. A. Lauffenburger. 1999. Quantitative relationship among integrin-ligand binding, adhesion, and signaling via focal adhesion kinase and extracellular signal-regulated kinase 2. *J. Biol. Chem*. 274:27119–27127.
9. Hao, N., M. Behar, …, H. G. Dohlman. 2007. Systems biology analysis of G protein and MAP kinase signaling in yeast. *Oncogene*. 26: 3254–3266.
10. Mettetal, J. T., D. Muzzey, …, A. van Oudenaarden. 2008. The frequency dependence of osmo-adaptation in *Saccharomyces cerevisiae*. *Science*. 319:482–484.
11. Drengstig, T., H. R. Ueda, and P. Ruoff. 2008. Predicting perfect adaptation motifs in reaction kinetic networks. *J. Phys. Chem. B*. 112:16752–16758.
12. Wilkie, J., M. Johnson, and K. Reza. 2002. Control Engineering. An Introductory Course. Palgrave, New York.
13. Yi, T. M., Y. Huang, …, J. Doyle. 2000. Robust perfect adaptation in bacterial chemotaxis through integral feedback control. *Proc. Natl. Acad. Sci. USA*. 97:4649–4653.
14. Ni, X. Y., T. Drengstig, and P. Ruoff. 2009. The control of the controller: molecular mechanisms for robust perfect adaptation and temperature compensation. *Biophys. J*. 97:1244–1253.
15. Novák, B., and J. J. Tyson. 2008. Design principles of biochemical oscillators. *Nat. Rev. Mol. Cell Biol*. 9:981–991.
16. Asher, G., J. Lotem, …, Y. Shaul. 2001. Regulation of p53 stability and p53-dependent apoptosis by NADH quinone oxidoreductase 1. *Proc. Natl. Acad. Sci. USA*. 98:1188–1193.
17. Leng, R. P., Y. Lin, …, S. Benchimol. 2003. Pirh2, a p53-induced ubiquitin-protein ligase, promotes p53 degradation. *Cell*. 112:779–791.
18. Dornan, D., I. Wertz, …, V. M. Dixit. 2004. The ubiquitin ligase COP1 is a critical negative regulator of p53. *Nature*. 429:86–92.
19. Asher, G., and Y. Shaul. 2005. p53 proteasomal degradation: poly-ubiquitination is not the whole story. *Cell Cycle*. 4:1015–1018.
20. Asher, G., and Y. Shaul. 2006. Ubiquitin-independent degradation: lessons from the p53 model. *Isr. Med. Assoc. J*. 8:229–232.
21. Yang, W., L. M. Rozan, …, W. S. El-Deiry. 2007. CARPs are ubiquitin ligases that promote MDM2-independent p53 and phospho-p53Ser^{20} degradation. *J. Biol. Chem*. 282:3273–3281.
22. Vogelstein, B., D. Lane, and A. J. Levine. 2000. Surfing the p53 network. *Nature*. 408:307–310.
23. Carr, A. M. 2000. Cell cycle. Piecing together the p53 puzzle. *Science*. 287:1765–1766.
24. Vousden, K. H., and X. Lu. 2002. Live or let die: the cell's response to p53. *Nat. Rev. Cancer*. 2:594–604.
25. Lev Bar-Or, R., R. Maya, …, M. Oren. 2000. Generation of oscillations by the p53-Mdm2 feedback loop: a theoretical and experimental study. *Proc. Natl. Acad. Sci. USA*. 97:11250–11255.
26. Lahav, G., N. Rosenfeld, …, U. Alon. 2004. Dynamics of the p53-Mdm2 feedback loop in individual cells. *Nat. Genet*. 36:147–150.
27. Geva-Zatorsky, N., N. Rosenfeld, …, U. Alon. 2006. Oscillations and variability in the p53 system. *Mol. Syst. Biol*. 2, 2006-0033.
28. Wilkinson, D. J. 2009. Stochastic modeling for quantitative description of heterogeneous biological systems. *Nat. Rev. Genet*. 10:122–133.
29. Wu, X., J. H. Bayle, …, A. J. Levine. 1993. The p53-mdm-2 autoregulatory feedback loop. *Genes Dev*. 7(7A):1126–1132.
30. Kubbutat, M. H., S. N. Jones, and K. H. Vousden. 1997. Regulation of p53 stability by Mdm2. *Nature*. 387:299–303.
31. Levine, A. J. 1997. p53, the cellular gatekeeper for growth and division. *Cell*. 88:323–331.
32. Jin, S., and A. J. Levine. 2001. The p53 functional circuit. *J. Cell Sci*. 114:4139–4140.
33. Brooks, C. L., and W. Gu. 2004. Dynamics in the p53-Mdm2 ubiquitination pathway. *Cell Cycle*. 3:895–899.
34. Candeias, M. M., L. Malbert-Colas, …, R. Fåhraeus. 2008. P53 mRNA controls p53 activity by managing Mdm2 functions. *Nat. Cell Biol*. 10:1098–1105.
35. Kruse, J. P., and W. Gu. 2009. Modes of p53 regulation. *Cell*. 137: 609–622.
36. Tai, E., and S. Benchimol. 2009. TRIMming p53 for ubiquitination. *Proc. Natl. Acad. Sci. USA*. 106:11431–11432.
37. Allton, K., A. K. Jain, …, M. C. Barton. 2009. Trim24 targets endogenous p53 for degradation. *Proc. Natl. Acad. Sci. USA*. 106: 11612–11616.
38. Momand, J., H. H. Wu, and G. Dasgupta. 2000. MDM2—master regulator of the p53 tumor suppressor protein. *Gene*. 242:15–29.
39. Fu, W., Q. Ma, …, W. Bai. 2009. MDM2 acts downstream of p53 as an E3 ligase to promote FOXO ubiquitination and degradation. *J. Biol. Chem*. 284:13987–14000.
40. Yu, G. W., S. Rudiger, …, A. R. Fersht. 2006. The central region of HDM2 provides a second binding site for p53. *Proc. Natl. Acad. Sci. USA*. 103:1227–1232.
41. Shirangi, T. R., A. Zaika, and U. M. Moll. 2002. Nuclear degradation of p53 occurs during down-regulation of the p53 response after DNA damage. *FASEB J*. 16:420–422.
42. Michael, D., and M. Oren. 2003. The p53-Mdm2 module and the ubiquitin system. *Semin. Cancer Biol*. 13:49–58.
43. Stommel, J. M., and G. M. Wahl. 2004. Accelerated MDM2 auto-degradation induced by DNA-damage kinases is required for p53 activation. *EMBO J*. 23:1547–1556.
44. Asher, G., J. Lotem, …, Y. Shaul. 2002. NQO1 stabilizes p53 through a distinct pathway. *Proc. Natl. Acad. Sci. USA*. 99:3099–3104.
45. Asher, G., J. Lotem, …, Y. Shaul. 2002. Mdm-2 and ubiquitin-independent p53 proteasomal degradation regulated by NQO1. *Proc. Natl. Acad. Sci. USA*. 99:13125–13130.
46. Das, S., S. A. Boswell, …, S. W. Lee. 2008. P53 promoter selection: choosing between life and death. *Cell Cycle*. 7:154–157.

47. Pietsch, E. C., S. M. Sykes, …, M. E. Murphy. 2008. The p53 family and programmed cell death. *Oncogene*. 27:6507–6521.

48. Tyson, J. J. 2004. Monitoring p53's pulse. *Nat. Genet*. 36:113–114.

49. Tyson, J. J. 2006. Another turn for p53. *Mol. Syst. Biol*. 2, 2006 -0032.

50. Lahav, G. 2008. Oscillations by the p53-Mdm2 feedback loop. *In* Cellular Oscillatory Mechanisms. M. Maroto and N. A. M. Monk, editors. Landes Bioscience and Springer Science & Business Media, Austin, TX.

51. Wee, K. B., U. Surana, and B. D. Aguda. 2009. Oscillations of the p53-Akt network: implications on cell survival and death. *PLoS One*. 4:e4407.

52. Kamijo, T., J. D. Weber, …, C. J. Sherr. 1998. Functional and physical interactions of the ARF tumor suppressor with p53 and Mdm2. *Proc. Natl. Acad. Sci. USA*. 95:8292–8297.

53. Borden, K. L. 2000. RING domains: master builders of molecular scaffolds? *J. Mol. Biol*. 295:1103–1112.

54. Savchenko, A., M. Yurchenko, …, E. Kashuba. 2009. Study on the spatial architecture of p53, MDM2, and p14ARF containing complexes. *Mol. Biotechnol*. 41:270–277.

55. Moore, J. W., and R. G. Pearson. 1981. Kinetics and Mechanism, 3rd Ed. John Wiley & Sons, New York.

56. Asher, G., J. Lotem, …, Y. Shaul. 2003. P53 hot-spot mutants are resistant to ubiquitin-independent degradation by increased binding to NAD(P)H:quinone oxidoreductase 1. *Proc. Natl. Acad. Sci. USA*. 100:15065–15070.

57. Gu, W., J. Luo, C. L. Brooks, A. Y. Nikolaev, and M. Li. 2004. Dynamics of the p53 acetylation pathway. *Novartis Found. Symp*. 259, 197–207, 223–225.

58. Jackson, M. W., and S. J. Berberich. 2000. MdmX protects p53 from Mdm2-mediated degradation. *Mol. Cell. Biol*. 20:1001–1007.

59. Press, W. H., B. P. Flannery, …, W. T. Vetterling. 1989. Numerical recipes. *In* The Art of Scientific Computing (Fortran Version). Cambridge University Press, New York.

60. Ma, J., J. D. Martin, …, Z. Lai. 2006. A second p53 binding site in the central domain of Mdm2 is essential for p53 ubiquitination. *Biochemistry*. 45:9238–9245.

61. Joseph, T. W., A. Zaika, and U. M. Moll. 2003. Nuclear and cytoplasmic degradation of endogenous p53 and HDM2 occurs during down-regulation of the p53 response after multiple types of DNA damage. *FASEB J*. 17:1622–1630.

62. Ma, L., J. Wagner, …, G. A. Stolovitzky. 2005. A plausible model for the digital response of p53 to DNA damage. *Proc. Natl. Acad. Sci. USA*. 102:14266–14271.

63. Sionov, R. V., and Y. Haupt. 1999. The cellular response to p53: the decision between life and death. *Oncogene*. 18:6145–6157.

64. Waxmann, D. 2000. Growth hormone pulse-activated STATS signaling: a unique regulatory mechanism governing sexual dimorphism of liver gene expression. Mechanisms and biological significance of pulsatile hormone secretion. *Novartis Found. Symp*. 227:61–81.

65. Goldbeter, A., and D. E. Koshland, Jr. 1981. An amplified sensitivity arising from covalent modification in biological systems. *Proc. Natl. Acad. Sci. USA*. 78:6840–6844.

66. Goldbeter, A. 2005. Zero-order switches and developmental thresholds. *Mol. Syst. Biol*. 1, 2005-0031.

67. Soyer, O. S., H. Kuwahara, and A. Csikász-Nagy. 2009. Regulating the total level of a signaling protein can vary its dynamics in a range from switch like ultrasensitivity to adaptive responses. *FEBS J*. 276: 3290–3298.

68. Sun, T., C. Chen, …, P. Shen. 2009. Modeling the role of p53 pulses in DNA damage- induced cell death decision. *BMC Bioinformatics*. 10:190.

69. Proctor, C. J., and D. A. Gray. 2008. Explaining oscillations and variability in the p53-Mdm2 system. *BMC Syst. Biol*. 2:75.

70. Zhang, T., P. Brazhnik, and J. J. Tyson. 2007. Exploring mechanisms of the DNA-damage response: p53 pulses and their possible relevance to apoptosis. *Cell Cycle*. 6:85–94.

71. Ciliberto, A., B. Novak, and J. J. Tyson. 2005. Steady states and oscillations in the p53/Mdm2 network. *Cell Cycle*. 4:488–493.

72. Wagner, J., L. Ma, …, G. A. Stolovitzky. 2005. p53-Mdm2 loop controlled by a balance of its feedback strength and effective dampening using ATM and delayed feedback. *Syst. Biol. (Stevenage)*. 152: 109–118.

73. Monk, N. A. 2003. Oscillatory expression of Hes1, p53, and NF-κB driven by transcriptional time delays. *Curr. Biol*. 13:1409–1413.

74. Qi, J. P., S. H. Shao, …, Y. Zhu. 2007. A mathematical model of P53 gene regulatory networks under radiotherapy. *Biosystems*. 90:698–706.

75. Cai, X., and Z. M. Yuan. 2009. Stochastic modeling and simulation of the p53-MDM2/MDMX loop. *J. Comput. Biol*. 16:917–933.

76. Goodwin, B. C. 1965. Oscillatory behavior in enzymatic control processes. *In* Advances in Enzyme Regulation, Vol. 3. G. Weber, editor. Pergamon Press, Oxford, UK.

77. Ruoff, P., and L. Rensing. 1996. The temperature-compensated Goodwin oscillator simulates many circadian clock properties. *J. Theor. Biol*. 179:275–285.

78. Ruoff, P., J. J. Loros, and J. C. Dunlap. 2005. The relationship between FRQ-protein stability and temperature compensation in the *Neurospora* circadian clock. *Proc. Natl. Acad. Sci. USA*. 102:17681–17686.

79. Ruoff, P. 2003. Modeling circadian clocks and temperature compensation. http://online.kitp.ucsb.edu/online/bionet03/ruoff/oh/47.html.

80. Friedman, N., S. Vardi, …, J. Stavans. 2005. Precise temporal modulation in the response of the SOS DNA repair network in individual bacteria. *PLoS Biol*. 3:e238.

81. Hoffmann, A., A. Levchenko, …, D. Baltimore. 2002. The IκB-NF-κB signaling module: temporal control and selective gene activation. *Science*. 298:1241–1245.

82. Nelson, D. E., A. E. Ihekwaba, …, M. R. White. 2004. Oscillations in NF-κB signaling control the dynamics of gene expression. *Science*. 306:704–708.

83. Ashall, L., C. A. Horton, …, M. R. White. 2009. Pulsatile stimulation determines timing and specificity of NF-κB-dependent transcription. *Science*. 324:242–246.